Persistence and breakdown of Airy beams driven by an initial nonlinearity

Article *in* Optics Letters · December 2010
DOI: 10.1364/OL.35.003952 · Source: PubMed

6 authors, including:

Yi Hu
105 PUBLICATIONS **1,436** CITATIONS

Weiyu Huang
Pall Corporation
15 PUBLICATIONS **363** CITATIONS

Peng Zhang
Changsha University of Science and Technology
30 PUBLICATIONS **933** CITATIONS

Cibo Lou
Nankai University
71 PUBLICATIONS **803** CITATIONS

Persistence and breakdown of Airy beams driven by an initial nonlinearity

Yi Hu,[1,2] Simon Huang,[1] Peng Zhang,[1] Cibo Lou,[2] Jingjun Xu,[2] and Zhigang Chen[1,2,*]

[1]*Department of Physics and Astronomy, San Francisco State University, San Francisco, California 94132, USA*

[2]*The Key Laboratory of Weak-Light Nonlinear Photonics, Ministry of Education and TEDA Applied Physics School, Nankai University, Tianjin 300457, China*

**Corresponding author: zhigang@sfsu.edu*

Received September 8, 2010; revised October 7, 2010; accepted October 19, 2010; posted October 26, 2010 (Doc. ID 134790); published November 23, 2010

We study the behavior of Airy beams propagating from a nonlinear medium to a linear medium. We show that an Airy beam initially driven by a self-defocusing nonlinearity experiences anomalous diffraction and can maintain its shape in subsequent propagation, but its intensity pattern and acceleration cannot persist when driven by a self-focusing nonlinearity. The unusual behavior of Airy beams is examined from their energy flow as well as the Brillouin zone spectrum of self-induced chirped photonic lattices.

OCIS codes: 190.4420, 050.1940, 350.5500.

Airy beams have recently attracted a great deal of interest [1–3] with many proposed applications [4–6]. Generation and control of Airy beams in an effective way is thus desirable. Apart from the linear control of Airy beams' ballistic trajectories [7,8], it has been demonstrated that nonlinearity can play nontrivial roles in both generation and control of Airy beams [9–11]. For example, by changing the phase-matching condition in a second harmonic generation process [9,10], one-dimensional Airy beams can be generated with controllable paths. In a photorefractive material with diffusion-dominated nonlinearity, self-trapping of Airy beams can be realized [11]. In this Letter, we study the transition of Airy beams from a nonlinear to a linear medium driven initially by a self-focusing or self-defocusing nonlinearity. Some unique behaviors of such nonlinearity-controlled Airy beams, including loss or persistence of acceleration and normal or anomalous diffraction are revealed. In particular, we found that an Airy beam under an initial self-defocusing nonlinearity exhibits anomalous diffraction and propagates robustly over a long distance after exiting the nonlinear medium, but it breaks down in both Airy beam pattern and acceleration when driven by a self-focusing nonlinearity. Our numerical results find good agreement with experimental observation.

Our experiments are performed in a biased 1-cm-long photorefractive SBN:60 crystal [Fig. 1(a)]. To create a truncated Airy beam, a spatial light modulator (SLM) is placed at the focal plane of the Fourier transform lens [2,3]. An extraordinarily polarized Airy beam ($\lambda = 532$ nm) is thus generated, propagating first through the biased crystal under the influence of photorefractive screening nonlinearity and then through air (free space) for another 1 cm. Solely by switching the polarity of the bias field, self-focusing and self-defocusing nonlinearity is achieved for nonlinear control of the Airy beam. The Airy beam patterns, along with **k**-space spectra are monitored by CCD cameras.

Typical experimental results are shown in Figs. 1(b), 1(c), and 1(d). When no bias field is present, the Airy beam undergoes linear propagation inside the crystal. (The photorefractive diffusion effect [11] can be neglected owing to the large size of the Airy beam used here—about 50 μm for the main lobe.) After another 1 cm of propagation in air, its main spot (or "head") is shifted along the vertical direction [Fig. 1(b2)] in comparison with that right at the existing face of the crystal [Fig. 1(b1)] owing to the transverse acceleration [1,2]. When a positive dc field of 4×10^4 V/m is applied, the Airy beam experiences a self-focusing nonlinearity and

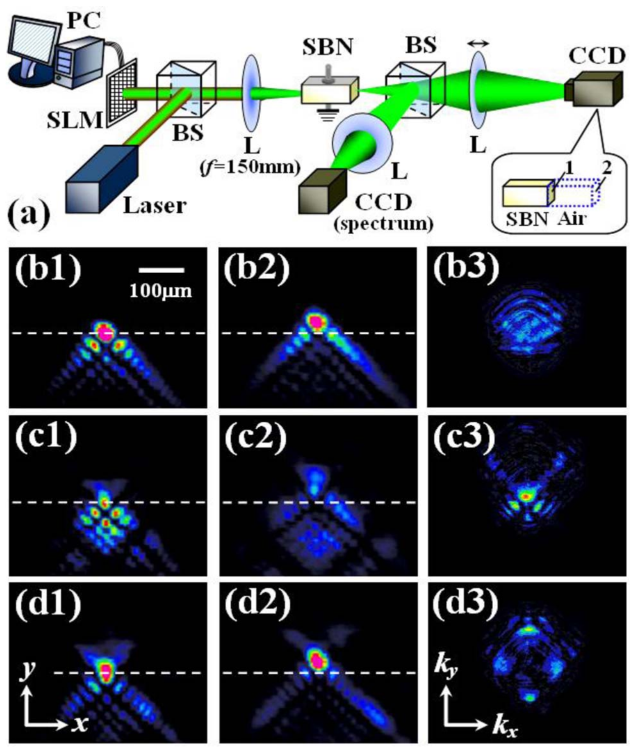

Fig. 1. (Color online) (a) Schematic of experimental setup. SLM, spatial light modulator; SBN, strontium–barium–niobate crystal; PC, personal computer; BS, beam splitter; L, Fourier transform lens. (b)–(d) Output intensity patterns of an Airy beam after 1 cm through crystal (first column) plus another 1 cm through air (second column) when (b) no nonlinearity, (c) self-focusing nonlinearity, and (d) self-defocusing nonlinearity are present. White dashed line marks the "head" position of the Airy beam at crystal output. The third column shows Fourier spectra of the Airy beam corresponding to the first column.

reduces its overall size with most of its energy distributed to the four spots close to the Airy “head” [Fig. 1(c1)]. In this case, the nonlinearity seems to cause stagnation of the Airy beam’s acceleration, and the subsequent free-space propagation shows that the Airy beam is strongly deformed by the nonlinearity [Fig. 1(c2)]. In addition, its **k**-space spectrum is “focused” toward the center [Fig. 1(c3)] as compared to the case without initial nonlinearity [Fig. 1(b3)], suggesting that the Airy beam exhibits normal diffraction. By reversing the polarity of the bias field (to -4×10^4 V/m) so the Airy beam experiences a self-defocusing nonlinearity, its nonlinear output [Fig. 1(d1)] and subsequent linear propagation [Fig. 1(d2)] behaves dramatically differently. The intensity profile of the Airy beam is less affected by the self-defocusing nonlinearity, and the peak intensity of the Airy beam after subsequent linear propagation in air is not decreased but rather increased while persistent in its acceleration [Fig. 1(d2)]. Furthermore, the Fourier spectrum reshapes into four major spots in **k**-space, as shown in Fig. 1(d3), resembling the Brillouin zone (BZ) spectrum and associated anomalous diffraction behavior in photonic lattices [12–14].

The above experimental observations can be corroborated with numerical simulations. Propagation of an Airy beam in a biased photorefractive crystal is described by the following nonlinear Schrödinger equation:

$$\frac{\partial U}{\partial z} = \frac{i}{2k_0 n_0}\left(\frac{\partial^2 U}{\partial x^2} + \frac{\partial^2 U}{\partial y^2}\right) + ik_0 \Delta n U, \tag{1}$$

where U is the wave function, k_0 is the vacuum wave vector, and $n_0 = 2.3$ is the unperturbed refractive index. In the biased crystal, the nonlinearity for an e-polarized beam can be determined by $\Delta n = -0.5 n_0^3 \gamma_{33} E_0/(1 + |U|^2)$, in which $\gamma_{33} = 280$ pm/V and E_0 is the amplitude of the bias field. The wave function of an input Airy beam can be expressed as $U(x, y, z = 0) = U_0 \mathrm{Ai}(X/x_0) \exp(\alpha X/x_0) \mathrm{Ai}(Y/y_0) \exp(\alpha Y/y_0)$, where U_0 is the amplitude; Ai denotes the Airy function; X and Y are equivalent to $(x + y)/\sqrt{2}$ and $(-x + y)/\sqrt{2}$, respectively; x_0 and y_0 are two scaling constants; and α is the decay factor for the truncated beam profile.

Numerical simulations are performed by solving Eq. (1) with the split-step beam propagation method. (Parameters U_0, x_0, and α are chosen as 7.3, 13.5 $\times 10^{-6}$, and 0.11, respectively.) Without the nonlinearity, i.e., $E_0 = 0$, the Airy beam is nearly unchanged after 2 cm linear propagation, and its output Fourier spectrum has a Gaussian-like shape. When $E_0 = +4 \times 10^4$ V/m is applied, it experiences a self-focusing nonlinearity, and its intensity concentrates mainly onto the four spots close to the Airy “head” while the “tails” get shorter [Fig. 2(a)], diverging even more in subsequent linear propagation [Fig. 2(b)]. The **k**-space spectrum reshapes asymmetrically into a bowtielike pattern, more localized toward the center [Fig. 2(c)]. The propagation can be better visualized from the side view evolution, as shown in Fig. 2(d), where the dashed curve marks the path of the same Airy beam without initial nonlinearity. The acceleration is reduced or lost as compared to the case without the nonlinear control. In Figs. 2(e) and 2(f), we plotted the transverse energy flow of the output beam corresponding to the areas marked in Figs. 2(a) and 2(b). Apparently, after initial nonlinear propagation, the direction of the energy flow goes toward all directions, suggesting that the phase of the Airy beam is destroyed by the self-focusing nonlinearity. Once the Airy beam is released into free space, it behaves more like a confined Gaussian beam, showing normal diffraction without evident acceleration.

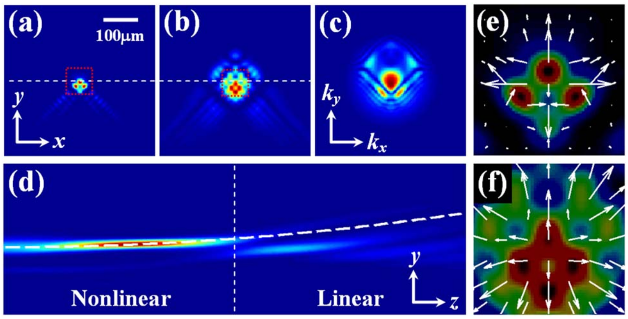

Fig. 2. (Color online) Numerical simulation of an Airy beam propagating under initial self-focusing nonlinearity. (a), (b) Transverse intensity patterns after (a) 1 cm through crystal plus (b) another 1 cm through air. (c) Fourier spectrum of the output Airy beam. (d) Side view of 2 cm propagation, where the dashed curve represents the trajectory of the Airy beam without initial nonlinearity. (e), (f) Calculated transverse energy flow around the main lobe corresponding to the square area shown in (a) and (b), respectively.

Now with a reversed bias field of $E_0 = -4 \times 10^4$ V/m, numerical results (Fig. 3) show that the Airy beam is somewhat expanded at the beginning owing to the self-defocusing nonlinearity, but its shape is nearly unchanged [Fig. 3(a)]. In contrast to the self-focusing case, the Airy beam persists in its intensity pattern and transverse acceleration during subsequent free-space propagation [Figs. 3(b) and 3(d)]. Furthermore, its power spectrum reshapes into a diamondlike pattern [Fig. 3(c)], resembling the first BZ [14] of an asymmetric square lattice. The energy flow of the Airy beam is also quite different from that in the self-focusing case, since the Poynting vectors of the Airy beam line up toward the same direction around the Airy “head” [Figs. 3(e) and 3(f)]. Counterintuitively, the peak intensity of the main lobe gets even stronger after subsequent linear propagation, as seen from the side view evolution [Fig. 3(d)]. This phenomenon suggests that the Airy beam might experience anomalous diffraction after initial self-defocusing nonlinearity, akin to that observed in photonic lattices [12,13].

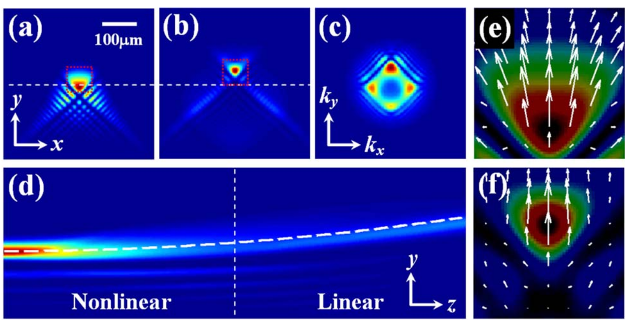

Fig. 3. (Color online) Numerical simulation of an Airy beam propagating under initial self-defocusing nonlinearity. Other description is the same as that for Fig. 2.

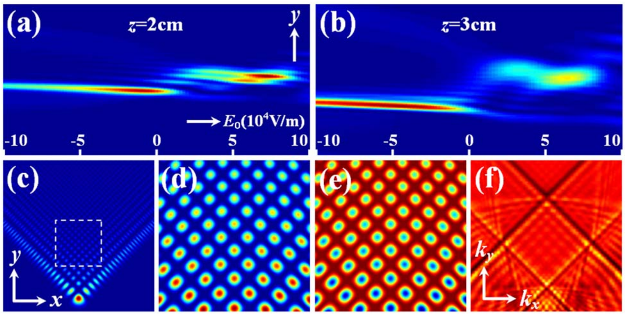

Fig. 4. (Color online) (a), (b) Plots of output intensity profiles along the y axis of an Airy beam as a function of the bias field after (a) 2 cm and (b) 3 cm of propagation, while the nonlinearity is on only for the first 1 cm. Positive (negative) values of E_0 correspond to self-focusing (self-defocusing) nonlinearity. (c) Transverse intensity pattern of a perfect Airy beam. (d) Zoom-in of nonuniform intensity pattern in the region marked by dashed square in (c). (e) Index lattice self-induced by the intensity pattern of (d) at $E_0 = -4 \times 10^4$ V/m. (f) Brillouin zone spectrum of the induced lattice of (e).

To get an idea of how much nonlinearity an Airy beam can withstand before it becomes deformed, we performed a series of simulations at different levels of nonlinearity as controlled by the bias field. The results are shown in Figs. 4(a) and 4(b), where the output transverse profiles along the y axis are plotted as a function of the bias field after 2 cm and 3 cm of propagation (only the first 1 cm with nonlinearity). Clearly, the Airy beam cannot maintain its shape after 2 cm of propagation even at a weak self-focusing nonlinearity (say, $E_0 = +10^4$ V/m), and it gets strongly deformed at higher bias fields. On the other hand, the Airy beam's main lobe withstands after 3 cm of propagation even at a strong self-defocusing nonlinearity (say, $E_0 = -10 \times 10^4$ V/m). In addition, from Fig. 4(b), it is evident that, under self-defocusing nonlinearity, the peak intensity of the Airy beam becomes much stronger than that in the linear case (i.e., $E_0 = 0$) after the same distance of propagation.

To better understand the "anomalous" behavior, let us take a close look at the diamondlike Fourier spectrum, as shown in Fig. 3(c). This spectrum is very similar to that of a gap soliton generated by balancing anomalous diffraction with a self-defocusing nonlinearity [14], for which the **k**-space spectrum populates mainly the four corners of the first BZ, indicating that the anomalous diffraction of the Airy beam might originate from the self-induced lattice structures. In Figs. 4(c) and 4(d), we zoom in the Airy beam intensity pattern not far from the "head," and it indeed exhibits a squarelike structure with nonuniform intensity distribution and lattice spacing. Under a self-defocusing nonlinearity, the Airy beam induces an index distribution akin to a nonuniform or chirped "backbone" lattice, as shown in Fig. 4(e). This self-induced lattice could exhibit properties similar to those of uniformed lattices [15] and thereby change the diffraction of the Airy beam. To visualize the BZ of the self-induced lattice, the BZ spectroscopy method is used to calculate the BZ spectrum of the induced lattice [16]; the result is displayed in Fig. 4(f). Clearly, the self-induced lattice of the Airy beam shows a BZ structure. Thus, the principle for anomalous diffraction observed here could be similar to that reported in [12,14,17].

In summary, we have studied nonlinearity-controlled persistence and breakdown of Airy beams. Our results bring about another possibility for control of Airy beams.

This work was supported by the National Science Foundation (NSF) and the Air Force Office of Scientific Research (USAFOSR) and by the 973 Program (2007CB613203), the 111 Project, the National Natural Science Foundation of China (NSFC), and the Program for Changjiang Scholars and Innovation Research Team (PCSIRT) in China. We thank D. N. Christodoulides for discussion.

References

1. G. A. Siviloglou and D. N. Christodoulides, Opt. Lett. **32**, 979 (2007).
2. G. A. Siviloglou, J. Broky, A. Dogariu, and D. N. Christodoulides, Phys. Rev. Lett. **99**, 213901 (2007).
3. J. Broky, G. A. Siviloglou, A. Dogariu, and D. N. Christodoulides, Opt. Express **16**, 12880 (2008).
4. J. Baumgartl, M. Mazilu, and K. Dholakia, Nat. Photon. **2**, 675 (2008).
5. P. Polynkin, M. Kolesik, J. V. Moloney, G. A. Siviloglou, and D. N. Christodoulides, Science **324**, 229 (2009).
6. A. Chong, W. Renninger, D. N. Christodoulides, and F. W. Wise, Nat. Photon. **4**, 103 (2010).
7. G. A. Siviloglou, J. Broky, A. Dogariu, and D. N. Christodoulides, Opt. Lett. **33**, 207 (2008).
8. Y. Hu, P. Zhang, C. Lou, S. Huang, J. Xu, and Z. Chen, Opt. Lett. **35**, 2260 (2010).
9. T. Ellenbogen, N. Voloch, A. Ganany-Padowicz, and A. Arie, Nat. Photon. **3**, 395 (2009).
10. I. Dolev, T. Ellenbogen, and A. Arie, Opt. Lett. **35**, 1581 (2010).
11. S. Jia, J. Lee, G. A. Siviloglou, D. N. Christodoulides, and J. W. Fleischer, Phys. Rev. Lett. **104**, 253904 (2010).
12. T. Pertsch, T. Zentgraf, U. Peschel, A. Bräuer, and F. Lederer, Phys. Rev. Lett. **88**, 093901 (2002).
13. P. Zhang, C. Lou, S. Liu, J. Zhao, J. Xu, and Z. Chen, Opt. Lett. **35**, 892 (2010).
14. X. Wang, A. Bezryadina, Z. Chen, K. G. Makris, D. N. Christodoulides, and G. I. Stegeman, Phys. Rev. Lett. **98**, 123903 (2007).
15. M. I. Molina, Y. V. Kartashov, L. Torner, and Y. S. Kivshar, Opt. Lett. **32**, 2668 (2007).
16. S. Liu, P. Zhang, X. Gan, F. Xiao, and J. Zhao, Appl. Phys. B **99**, 727 (2010).
17. C. Lou, X. Wang, J. Xu, Z. Chen, and J. Yang, Phys. Rev. Lett. **98**, 213903 (2007).